Research Article

Received: 21 September 2022 Revised: 27 December 2022 Accepted article published: 23 January 2023 Published online in Wiley Online Library: 2 February 2023

(wileyonlinelibrary.com) DOI 10.1002/ps.7375

Quantitative transcriptomic and proteomic analyses reveal the potential maintenance mechanism of female adult reproductive diapause in *Chrysoperla nipponensis*

Zhen-Zhen Chen,[a] Xiao Wang,[a] Xue Kong,[a] Yue-Ming Zhao,[a] Ming-Hui Xu,[a] Yu-Qing Gao,[a] Hai-Yi Huang,[a] Fang-Hua Liu,[b] Su Wang,[c] Yong-Yu Xu[a*] and Zhi-Wei Kang[b*]

Abstract

BACKGROUND: The green lacewing *Chrysoperla nipponensis* is an important natural enemy of many insect pests and exhibits reproductive diapause to overwinter. Our previous studies showed that adult *C. nipponensis* enters reproductive diapause under a short-day photoperiod. However, the molecular mechanism underlying diapause maintenance in *C. nipponensis* is still unknown.

RESULTS: The total lipid and triglyceride content showed the reservation and degradation of energy during diapause in *C. nipponensis*. Thus, we performed combined transcriptomic and proteomic analyses of female reproductive diapause in *C. nipponensis* at three ecophysiological phases (initiation, maintenance and termination). A total of 64 388 unigenes and 5532 proteins were identified from the transcriptome and proteome. In-depth dissection of the gene-expression dynamics revealed that differentially expressed genes and proteins were predominately involved in the lipid and carbohydrate metabolic pathways, in particular fatty acid metabolism, metabolic pathways and the citrate cycle. Among of these genes, *TIM*, *CLK*, *JHAMT2*, *PMK*, *HMGS*, *HMGR*, *FKBP39*, *Kr-h1*, *Phm*, *ECR*, *IR1*, *ILP3*, *ILP4*, *mTOR*, *ACC*, *LSD1* and *LSD2* were differentially expressed in diapause and non-diapause female adults of *C. nipponensis*. The expression patterns of these genes were consistent with the occurrence of vitellogenesis and expression of either *Vg* or *VgR*.

CONCLUSION: Our findings indicated that diapause adult *C. nipponensis* accumulate energy resources to overwinter. Transcriptomic and proteomic analyses suggested candidate key genes involved in the maintenance of *C. nipponensis* during adult reproductive diapause. Taken together, these results provide in-depth knowledge to understand the maintenance mechanism of *C. nipponensis* during adult reproductive diapause.

Supporting information may be found in the online version of this article.

Keywords: *Chrysoperla nipponensis*; reproductive diapause; proteome; transcriptome; diapause maintenance

1 INTRODUCTION

Diapause is an important adaptative strategy by which many insects survive in adverse environmental conditions.[1,2] There are two types of diapause: facultative, which is elicited by environmental cues (commonly photoperiod and temperature); and obligatory, which occurs at a specific development stage with no requirement for a token stimulus.[1,3,4] *Bactrocera minax* and *Leguminivora glycinivorella* enter obligatory pupal diapause every generation,[3,4] whereas short daylengths and low temperatures are required for diapause induction in *Laodelphax striatellus*.[5] In *Colaphellus bowringi*, larval experience under a long photoperiod at 25°C causes facultative reproductive diapause in adults.[6]

Because feeding is often stopped or reduced, sufficient nutrient reserves are critical for successful overwintering and diapause.[7] Triacylglycerides are the dominant form of reserved energy

* *Correspondence to: Yong-Yu Xu, College of Plant Protection, Shandong Agricultural University, Tai'an, Shandong, China. E-mail: xuyy@sdau.edu.cn Zhi-Wei Kang, School of Life Sciences, Institutes of Life Science and Green Development, Hebei University, Baoding 071002, China. E-mail: zwkang2010@126.com*

Zhen-Zhen Chen, Xiao Wang and Xue Kong contributed equally to this study.

a *College of Plant Protection, Shandong Agricultural University, Tai'an, China*

b *School of Life Sciences, Institutes of Life Science and Green Development, Hebei University, Baoding, China*

c *Beijing Key Laboratory of Environment Friendly Management on Fruit Diseases and Pests in North China, Institute of Plant Protection, Beijing Academy of Agriculture and Forestry Sciences, Beijing, China*

substrates in diapause insects.[1,2,8] In *Harmonia axyridis*, the daily feeding amount of both pre-diapause males and females was significantly lower than that of both pre-reproductive male and female adults.[9] Meanwhile, pre-diapause female adults reserved more carbohydrates and lipids, whereas pre-diapause male accumulated only more carbohydrates.[9] Similarly, pre-diapause females of *Colaphellus bowringi* synthesized and accumulated more triacylglycerol (TAG) in the fat body, whereas reproductive females channeled nutrients into proteins and carbohydrates for egg reproduction.[7] Several studies have revealed that juvenile hormone (JH) and the insulin signaling pathway are the key regulators involved in diapause induction, maintenance, and termination.[1,10,11]

JH is one of the most important hormones involved in various insect physiological processes, including insect development, metamorphosis, diapause, reproduction and immunity.[1,11,12] In *H. axyridis* and *Bombus terrestris*, diapause adults had a lower JH titer than non-diapause adults.[13,14] Furthermore, cultured corpora allata dissected from non-diapausing females of *Culex pipiens* secreted more JH than corpora allata from diapause females.[15] Topical application or injection of synthetic JH and JH analogs can rescue diapause adults from reproductive arrest in many insect species including *Colaphellus bowringi*, *H. axyridis*, *Culex pipiens* and *B. terrestris*.[16,17] Knockdown of juvenile hormone acid methyltransferase (*JHAMT*) in *Leptinotarsa decemlineata*, *Sogatella furcifera*, *H. axyridis*, *Colaphellus bowringi* and *Blattella germanica* leads to ovarian development arrest.[16,18–20] Besides the JH biosynthesis genes, JH receptor methoprene-tolerant (*Met*) and JH downstream transcription factor krüppel homolog 1 (*Kr-h1*) are also involved in the insect diapause.[17,21,22] Similar to the diapause state, depletion of *Met* in *Pyrrhocoris apterus*, *Colaphellus bowringi*, *Galeruca daurica* and *H. axyridis* resulted in ovarian development arrest.[16,17,21–23] Consistent with this, silencing of *Kr-h1* prevented ovarian development in *Nilaparvata lugens*, *Locusta migratoria* and *Colaphellus bowringi*.[13,24,25] Insulin signaling is another well-documented regulator of insect diapause.[1,26,27] Injection of bovine insulin into diapausing pupae of *Pieris brassicae* and *Antheraea pernyi*, or human insulin into diapause queens of *B. terrestris* terminated diapause.[13,28,29] Inhibiting the expression of insulin receptors (*InRs*) and insulin-like peptides (*ILPs*) in *Culex pipiens* and *Chrysopa pallens* blocks ovarian development.[27,30,31] JH III and methoprene, a JH analog, can rescue *ILP* and *InR* RNA interference (RNAi) caused ovarian arrest in *Culex pipiens*, respectively.[27,30] Furthermore, inhibiting expression of *FOXO*, the downstream gene of insulin signaling, significantly influenced the storage of nutrients in diapause *Culex pipiens* adults and *L. striatellus* nymph.[27,32]

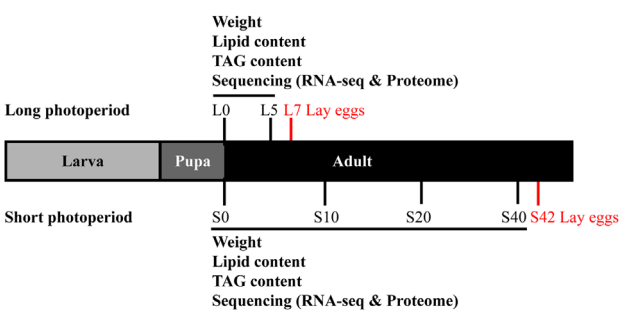

FIGURE 1. Illustration of the experimental design. L, long photoperiod; S, short photoperiod.

The green lacewing, *Chrysoperla nipponensis* Okamoto (Neuroptera: Chrysopidae), is an important biological control agent for numerous agricultural and forest pests that has a wide geographic distribution and is highly adaptable.[33–36] The maximum predation number of first, second and third instars of *C. nipponensis* on *Aphis gossypii* within 24 h was 13.8, 65.9, and 114.6.[34] In temperate regions, female adults of *C. nipponensis* enter facultative reproductive diapause during early winter and start reproduction in spring of the following year.[33,37] Usually, *C. nipponensis* diapause lasts several months. Chen *et al*. found that photoperiod was the most important environmental factor in the induction and maintenance of reproductive diapause in *C. nipponensis*.[33] Female adults of *C. nipponensis* enter reproductive diapause with obvious changes in body color (reproductive females are green; reproductive diapause females are brown and yellow) when reared on a short photoperiod under laboratory condition.[38,39] However, there is no information about the molecular mechanisms of reproductive diapause in *C. nipponensis*. Because of the increasing importance of *C. nipponensis* as a biological agent, understanding the molecular regulation of this crucial life history trait could help us improve the mass storage and shipment of this insect. Thus, in this study, we first quantified the weight, lipid, and TAG content of *C. nipponensis* females during overwintering in a field population and at three different diapause statuses in a laboratory colony (short photoperiod-induced reproductive diapause). We then conducted transcriptome and proteome analysis of *C. nipponensis* females at three different diapause statuses in a laboratory colony to explore the potential maintenance mechanisms of *C. nipponensis* females during adult reproductive diapause at the molecular level.

2 MATERIAL AND METHODS

2.1 *C. nipponensis* rearing and sample preparation

To quantify the weight, total lipid, and TAG content of *C. nipponensis* during winter, we collected female adults of *C. nipponensis* at the campus of Shandong Agricultural University (36°20′ N, 117°13'E, Tai'an, Shandong, China) from September 2019 to June 2020.

Laboratory colonies of *C. nipponensis* were maintained in an artificial climate chamber (RXZ-380C, Ningbo Dongnan Instrument Co.) at 25 ± 1°C and a 15:9 h light/dark photoperiod, as described in our previous study.[33] For diapause induction, eggs were transferred to fingertip tubes (1 cm in diameter and 7 cm in height) and kept under a short photoperiod (9:15 h light/dark photoperiod) and 25 ± 1°C until sample collection (Figure 1) at the adult stages (S0, day 0; S10, day 10; S20, day 20; S40, day 40 after eclosion). Adults that emerged from the colony under normal conditions (long photoperiod 15:9 h light/dark and 25 ± 1°C) were used as a positive control and collected at day 0 (L0) and 5 (L5) after adult eclosion (Figure 1).

2.2 Measurement of weight, total lipid, and TAG content

The fresh weight of adults at the sample collection time points was measured using an electronic microbalance (Sartorius Analystic; $N \geq 25$). *C. nipponensis* adults were dried in an oven (Yiheng) at 60°C for 72 h. After drying, dry weight was measured using the electronic microbalance (Sartorius Analystic; $N \geq 25$). A one-way analysis of variance (ANOVA) was used to analyze the differences among the sample times followed by separation of means using Fisher's protected least significant difference (LSD) test at $p = 0.05$ (SPSS 22.0, SPSS Inc.).

The dry weight of each adult female (DW) was recorded at each time point to measure the total lipid content. Meanwhile, each fresh adult was transferred into a new Eppendorf tube, weighed (W1), and then homogenized in 500 µl of chloroform/methanol (2:1). All samples were centrifuged at 2600 *g* for 10 min, and the pellets were kept. The previous step was repeated and samples were dried in an oven at 60°C for 72 h. The weights of dried samples (W2) were measured using an electronic microbalance (Sartorius Analystic; $N \geq 25$). The total lipid content was calculated as (W1 − W2)/DW. TAG content was determined using a triglyceride assay kit (code A110-2-1; Nanjing Jiancheng Bioengineering Institute) following the manufacturer's protocol. The total lipid and TAG content of 30 female adults was measured for each time point. Differences in total lipid and TAG among treatments were also determined by ANOVA with LSD test at $p = 0.05$ (SPSS 22.0, SPSS Inc.).

2.3 RNA extraction and transcriptome sequencing

The total RNA of all samples (three female adults per replicate and three biological replicates per treatment) was extracted using RNAiso plus (code 9109; Takara Bio) according to the manufacturer's protocol. The quantity and quality of RNA were assessed using Nanodrop (Life Technologies) and Agilent 2100 (Agilent Technologies) at Jingjie PTM BioLabs. Synthesis of complementary DNA (cDNA) and the sequence of library preparations on the Illumina Novaseq platform (Illumina) were finished by Jingjie PTM BioLabs with 150 bp paired-end reads. Quality control, de novo transcriptome assembly using Trinity, gene functional annotation, and differential expression analysis by DESeq2 were accomplished as previously described.[40,41] Heat maps were constructed based on the differential expression analysis using pheatmap in R 4.0.4.[42,43] The sequences reported here have been deposited in the Genbank SRA database (BioProject ID: PRJNA788306).

2.4 Tandem mass tag (TMT)/Isobaric tags for relative and absolute quantitation (iTRAQ)

The sample was ground into a powder using liquid nitrogen and then transferred to a 5 ml centrifuge tube with 4 vol. of lysis buffer (8 M urea, 1% Protease Inhibitor Cocktail). All samples were sonicated three times on ice using a high-intensity ultrasonic processor (Scientz). The remaining debris was removed by centrifugation at 12 000 *g* at 4°C for 10 min. The supernatant was collected, and the protein concentration was determined with a BCA kit (Thermo Fisher Scientific) according to the manufacturer's instructions. After protein extraction, the samples were digested with trypsin at 1:50 for the first digestion (12 h) and 1:100 for the second digestion (4 h). All samples were desalted and vacuum-dried, followed by tandem mass tag (TMT)/Isobaric tags for relative and absolute quantitation (iTRAQ) labeling using TMT/iTRAQ kit (Thermo Fisher Scientific). Liquid chromatography–tandem mass spectrometry analysis, database search, and bioinformatic analyses were conducted by Jingjie PTM BioLabs using standard procedures.[13] Proteome data are available via ProteomeXchange with identifier PXD030378 (http://www.ebi.ac.uk/pride).

2.5 Validation of selected genes by quantitative polymerase chain reaction

Quantitative polymerase chain reaction (qPCR) analysis of several selected genes was performed using a CFX96 Touch Real-Time PCR Detection System (Bio-Rad) to verify the transcriptomic and proteomic results. The total RNA of all samples (three female adults per replicate and three biological replicates per treatment) was extracted using RNAiso plus (code 9109; Takara Bio) as described above. cDNA was synthesized from total RNA using a FastQuant RT Kit (with gDNase) (code KR106; Tiangen) according to the standard manufacturer's protocol. The primers used are provided in Table S1. Twenty microliters of the qPCR mixture contained 2 µl of cDNA, 0.8 µl of each primer, 6.4 µl of ddH_2O and 10 µl of TB Green (code RR420W; Takara Bio). The qPCR program and statistical analyses are referred to in Kang et al.[44] and Wang et al.[38]

2.6 Effects of topical application of JH III on preoviposition period and fecundity of female diapause adults

Newly emerged female adults under the short photoperiod condition were collected and incubated at 4°C for 30 min to reduce

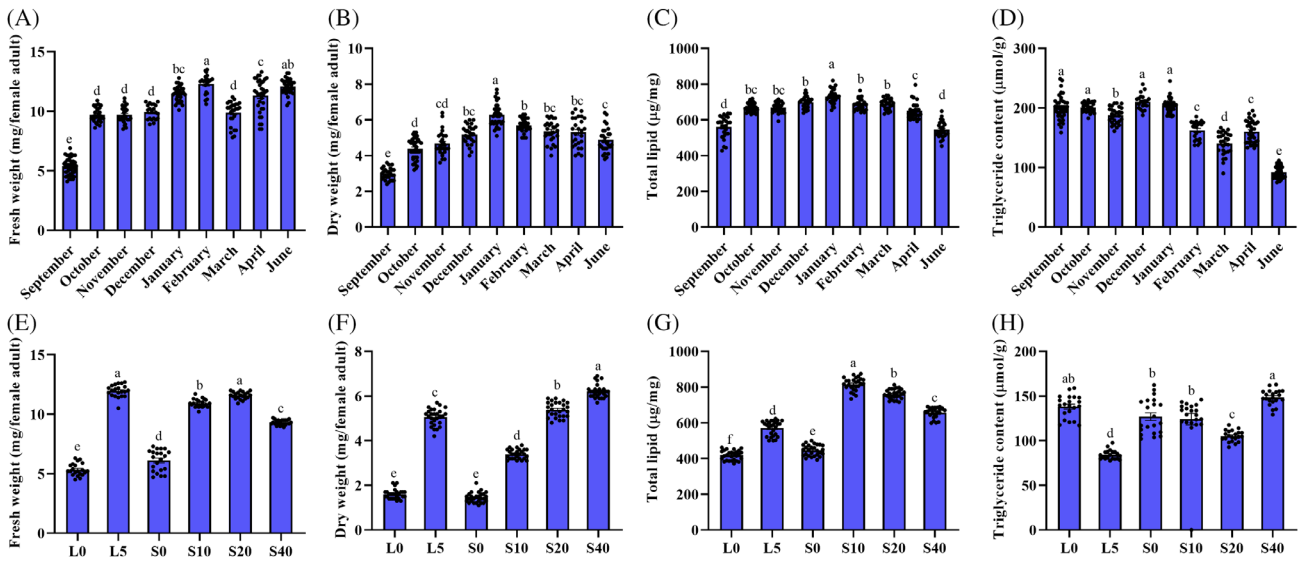

FIGURE 2. Changes in weight, total lipid and triacylglycerol (TAG) content during overwintering and at different diapause phases. L, long photoperiod; S, short photoperiod.

(A)

	Total sequence number	Total sequence length	Max length	Min length	Average length	N50	N90	GC percent
Unigenes	64388	44726244	33101	197	694	2055	233	33.13%
Transcripts	71999	57382674	33101	194	796	2274	239	32.89%

(B)

Total spectrum	Matched spectrum	Peptides	Unique peptides	Identified proteins	Quantifiable proteins
812156	182261 (22.4%)	97214	95767	5532	4942

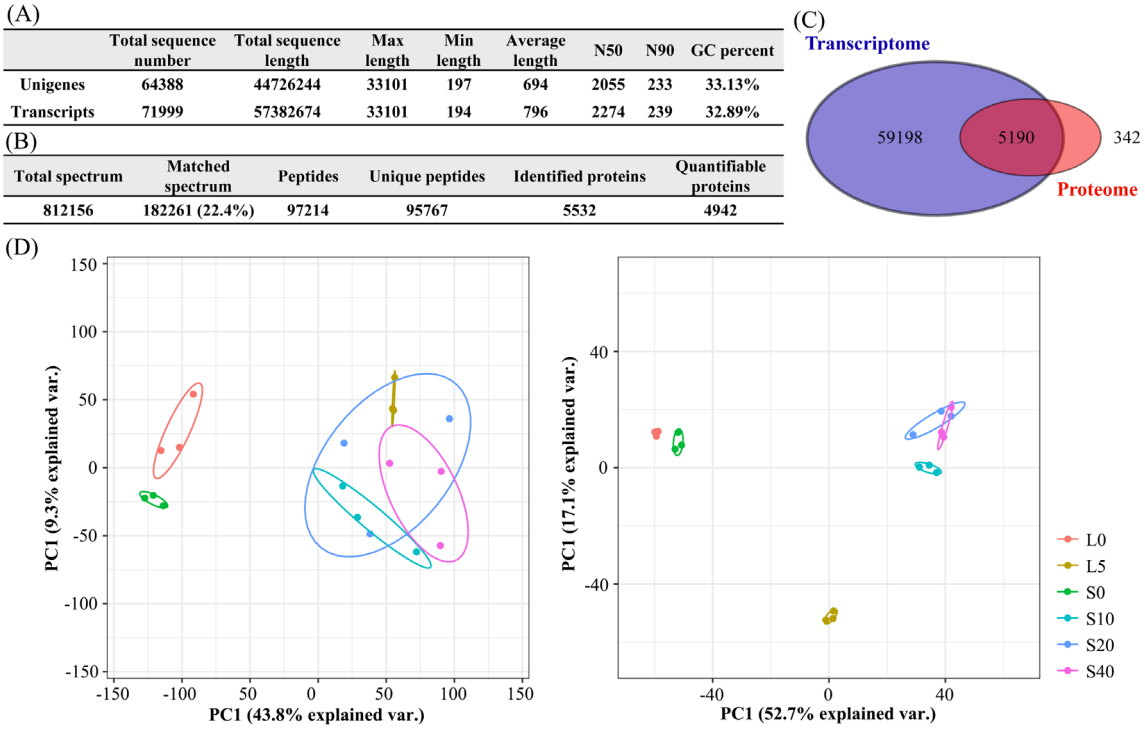

FIGURE 3. Overall transcriptomic and proteomic analyses of *Chrysoperla nipponensis* female during adult reproductive diapause. (A,B) Basic information about transcriptome (A) and proteome (B). (C) Overlap of identified unigenes and proteins between transcriptome and proteome. (D) Principal components analysis (PCA) analysis of the abundance of transcripts from transcriptomes (left) and proteins from proteome (right).

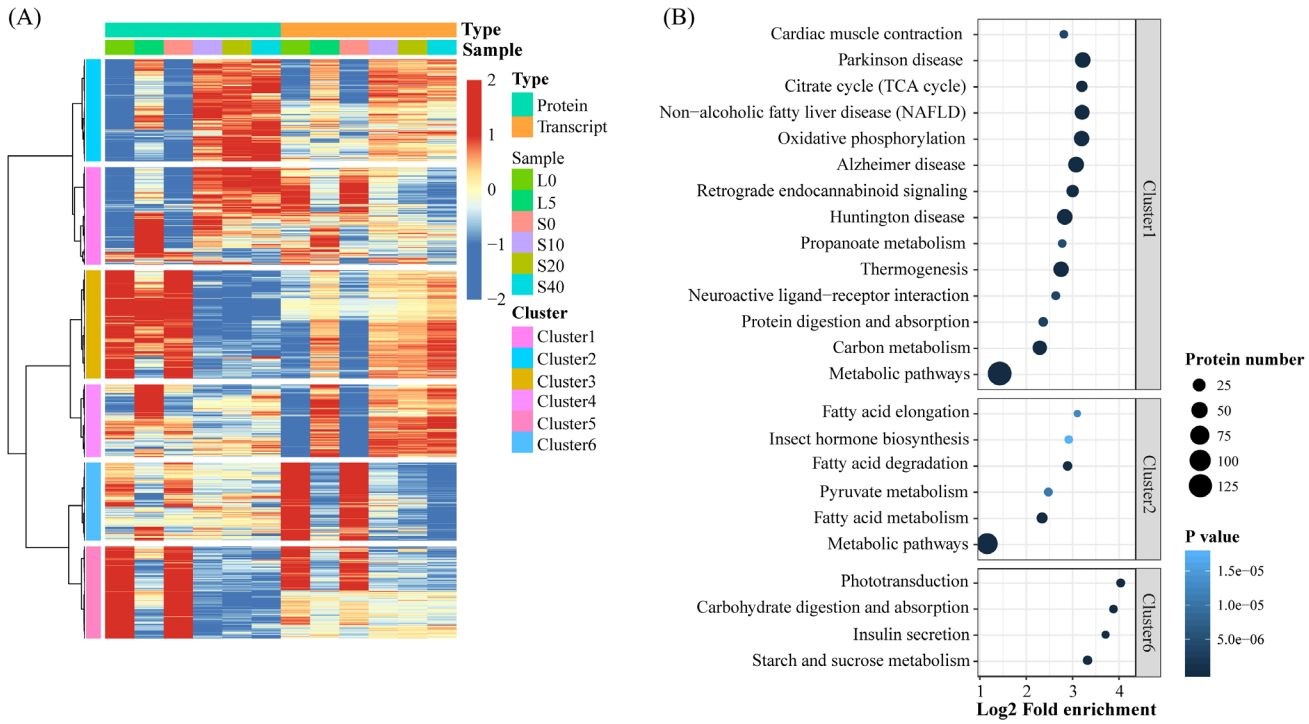

FIGURE 4. Differentially expressed genes and proteins of *Chrysoperla nipponensis* female during adult reproductive diapause. (A) Stratified cluster heat map of transcriptomic and proteomic data based on their abundance correlation. (B) KEGG pathway of clusters 1, 2 and 6. Data are presented as means of three independent samples.

their activity. Fifteen micrograms of JH III (E589400, Toronto Research Chemicals) or acetone were applied to the abdomen through topical application using a microinjector. All treated females were maintained as described above. The pre-oviposition period and fecundity were recorded. Females reared under long photoperiods were used as a positive control. Differences in pre-

TABLE 1. Differentially expressed genes and proteins

	Transcriptome		Proteome	
Treatment	Upregulated	Downregulated	Upregulated	Downregulated
S0 vs. L0	57	33	76	43
L5 vs. L0	2010	3332	916	887
S10 vs. S0	1969	2685	882	1267
S20 vs. S0	2102	2260	961	1353
S40 vs. S0	2611	3133	928	1279

TABLE 2. Putative circadian clock genes of *Chrysoperla nipponensis*

Gene ID	Gene name	Best blast	Accession	e-value	Percent identity
DN328_c3_g1	*PER*	Period circadian protein [*Chrysoperla carnea*]	XP_044728341.1	0	95.48
DN1200_c22_g1	*CLK*	PREDICTED: clock isoform X1 [*Tribolium castaneum*]	XP_008199501.1	0	59.84
DN857_c2_g2	*TIM*	Protein timeless [*Chrysoperla carnea*]	XP_044729573.1	0	99.50
DN3077_c0_g1	*CYC*	Protein cycle isoform X1 [*Chrysoperla carnea*]	XP_044733956.1	0	99.86
DN862_c39_g1	*CRY1*	Cryptochrome-1 [*Chrysoperla carnea*]	XP_044734495.1	0	99.07

oviposition period and fecundity among the treatments were determined by ANOVA with LSD test at $p = 0.05$ (SPSS 22.0, SPSS Inc.).

3 RESULTS

3.1 Changes in weight, total lipid, and TAG content

The lowest temperature in winter 2019/2020 was −9°C on 31 December (Figure S1). Between 15 November and 8 February, mean and lowest temperatures were below 10°C and 0°C, respectively (Figure S1). The fresh weight (df = 8; $F = 234.6$; $p < 0.001$) and dry weight (df = 8; $F = 69.72$; $p < 0.001$) of *C. nipponensis* increased, reaching the highest values in January (Figure 2). There were obvious accumulations of total lipid (df = 8; $F = 75.26$; $p < 0.001$) and TAG content (df = 8; $F = 208.6$; $p < 0.001$) during overwintering (Figure 2). In the laboratory, the fresh weight (df = 5; $F = 644.1$; $p < 0.001$) and dry weight (df = 5; $F = 1370$; $p < 0.001$) of female adults were increased after eclosion in both diapause and non-diapause female adults, whereas the dry weight of diapause female adults increased more slowly than that of non-diapause female adults (Figure 2). Similarly, the total lipid content (df = 5; $F = 695.3$; $p < 0.001$) of diapause female adults at days 10, 20 and 40 were significantly higher than for other treatments (Figure 2). TAG content (df = 5; $F = 41.83$; $p < 0.001$) of newly emerged adults and diapause female adults was significantly higher than that in non-diapause female adult at day 5 (Figure 2).

3.2 Overall results of the transcriptomic and proteomic analysis

In this study, we identified 71 999 transcripts, 64 388 unigenes, and 5532 proteins (Figure 3A,B). Among these, 5190 genes were found in both the transcriptome and proteome, whereas 342 proteins were found only in the proteome (Figure 3C). Separation analyses of the proteome and transcriptome showed a clear separation among these treatments with 53.1% (transcriptome) and 69.8% (proteome) variation (Figure 3B). However, there was a noticeable clustering difference between the transcriptome and proteome (Figure 3B). At the transcriptional level, L5 was clustered with S10, S20 and S40, but was separated from the two clusters of L0 and S0 (Figure 3B, left). At the proteomic level, L5 formed as one separate cluster, whereas S10, S20 and S40 were also clustered together (Figure 3B, right). These results indicated that: (1) the changes in transcripts at L5, S10, S20, and S40 differed considerably from newly emerged adults at L0 and S0; and (2) the proteomic changes in S10, S20, and S40 appeared to be in a different direction from the changes observed in L5.

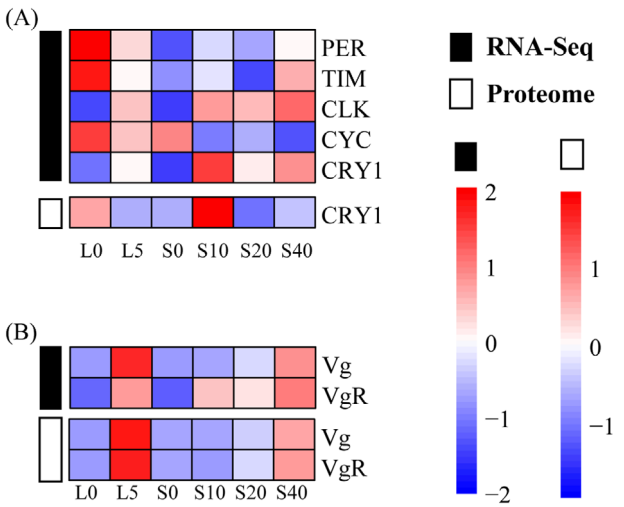

FIGURE 5. Heat maps of circadian clock genes at transcript and protein levels of *Chrysoperla nipponensis* female during adult reproductive diapause. (A) Circadian clock genes. (B) Marker genes (*Vg* and *VgR*). Data are presented as means of three independent samples.

These identified transcripts and proteins were clustered into six groups based on hierarchical clustering analysis of transcriptomic and proteomic data (Figures 4A and S2). In addition, proteins in

TABLE 3. Putative genes involved in juvenile hormone, molting hormone and insulin/TOR pathway of *Chrysoperla nipponensis*

Gene ID	Gene name	Best blast	Accession	e-value	Percent identity
Juvenile Hormone					
JH synthesis					
DN199_c0_g2	*HMGS*	Hydroxymethylglutaryl-CoA synthase 1 [*Chrysoperla carnea*]	XP_044734844.1	0	99.78
DN55204_c0_g1	*HMGR*	3-Hydroxy-3-methylglutaryl-coenzyme A reductase [*Chrysoperla carnea*]	XP_044732135.1	0	99.88
DN51455_c0_g1	*MevK*	Mevalonate kinase [*Chrysoperla carnea*]	XP_044740165.1	0	99.74
DN14374_c0_g1	*PMK*	Probable phosphomevalonate kinase [*Chrysoperla carnea*]	XP_044734816.1	3.00 e^{-62}	95.92
DN22501_c0_g1	*PPMD*	Diphosphomevalonate decarboxylase isoform X1 [*Chrysoperla carnea*]	XP_044732780.1	0	99.48
DN2112_c0_g1	*FOLD1*	Farnesol dehydrogenase-like [*Chrysoperla carnea*]	XP_044728984.1	0	98.42
DN695_c19_g1	*FOLD2*	Farnesol dehydrogenase-like [*Chrysoperla carnea*]	XP_044733151.1	0	100
DN1091_c0_g1	*FOLD3*	Farnesol dehydrogenase-like [*Chrysoperla carnea*]	XP_044731920.1	2.00 e^{-177}	98.77
DN2600_c0_g1	*FOLD4*	Farnesol dehydrogenase-like [*Chrysoperla carnea*]	XP_044731919.1	1.00 e^{-177}	97.97
DN113_c1_g2	*FOLD5*	Farnesol dehydrogenase-like [*Chrysoperla carnea*]	XP_044731918.1	3.00 e^{-179}	98.79
DN1970_c0_g1	*FOLD6*	Farnesol dehydrogenase-like [*Chrysoperla carnea*]	XP_044733703.1	2.00 e^{-173}	97.11
DN3743_c0_g2	*FOLD7*	Farnesol dehydrogenase-like [*Chrysoperla carnea*]	XP_044731173.1	0	99.21
DN6011_c0_g5	*FOLD8*	Farnesol dehydrogenase-like [*Chrysoperla carnea*]	XP_044729972.1	0	100
DN14092_c0_g1	*JHAMT1*	Juvenile hormone acid *O*-methyltransferase-like [*Photinus pyralis*]	XP_031340281.1	2.00 e^{-71}	40.79
DN4543_c0_g1	*JHAMT2*	Juvenile hormone acid *O*-methyltransferase-like [*Onthophagus taurus*]	XP_022905522.1	2.00 e^{-70}	40.29
DN1134_c0_g1	*CYP15A1*	Methyl farnesoate epoxidase-like [*Chrysoperla carnea*]	XP_044731953.1	0	98.18
JH sequestration					
DN84855_c0_g1	*HEX1*	Hexamerin-1.1-like [*Ctenocephalides felis*]	XP_026475430.1	0	47.90
DN14569_c0_g1	*HEX2*	Hexamerin-1.1-like [*Anopheles albimanus*]	XP_035777010.1	7.00 e^{-160}	50.00
JH degradation					
DN855_c0_g1	*JHE1*	Esterase-6-like protein [*Tribolium castaneum*]	EFA06757.1	7.00 e^{-67}	56.19
DN858_c1_g2	*JHE2*	Carboxylesterase 11 [*Holotrichia parallela*]	QIK02111.1	4.00 e^{-143}	43.87
DN72197_c0_g1	*JHE3*	PREDICTED: esterase B1 [*Tribolium castaneum*]	XP_015838352.1	1.00 e^{-47}	53.05
DN29606_c0_g1	*JHEH1*	Juvenile hormone epoxide hydrolase 1 [*Cryptotermes secundus*]	XP_023724762.1	0	58.59
DN3953_c2_g1	*JHEH2*	Epoxide hydrolase 3 isoform X1 [*Cryptotermes secundus*]	XP_023705967.1	2.00 e^{-107}	45.54
JH reception mechanism					
DN705_c1_g1	*Met*	PREDICTED: methoprene-tolerant isoform X1 [*Tribolium castaneum*]	XP_008191439.1	4.00 e^{-122}	48.17
DN198_c11_g1	*Cdh64*	Myophilin-like isoform X1 [*Ctenocephalides felis*]	XP_026472987.1	3.00 e^{-115}	85.11
DN17197_c1_g1	*FKBP39*	46 kDa FK506-binding nuclear protein isoform X1 [*Maniola hyperantus*]	XP_034833396.1	2.00 e^{-59}	64.90
Downstream of JH pathway					
DN1828_c2_g1	*Kr-h1*	Krueppel homolog 1-like isoform X2 [*Photinus pyralis*]	XP_031343195.1	5.00 e^{-135}	69.23
Molting Hormone					
Ecdysone synthesis					
DN8286_c0_g1	*Phm*	Cytochrome P450 306a1 [*Leptinotarsa decemlineata*]	AGT57833.1	0	53.53
DN3502_c4_g1	*Sad*	PREDICTED: cytochrome P450 315a1, mitochondrial [*Tribolium castaneum*]	XP_008193656.1	5.00 e^{-145}	44.24
ECD reception mechanism					
DN4528_c1_g1	*ECR*	Ecdysone receptor isoform X1 [*Zootermopsis nevadensis*]	XP_021939014.1	0	78.80
Downstream of ECD pathway					

TABLE 3. Continued

Gene ID	Gene name	Best blast	Accession	e-value	Percent identity
DN2237_c0_g1	*E74*	Ecdysone-induced protein 74EF-like [*Agrilus planipennis*]	XP_025829364.1	2.00 e^{-146}	51.08
DN3559_c0_g2	*E75*	Ecdysone-inducible protein E75 isoform X4 [*Cryptotermes secundus*]	XP_023709203.1	0	69.68
Insulin/TOR					
DN2572_c1_g1	*ILP3*	Insulin-like peptide 3 [*Chrysopa pallens*]	QBS36241.1	3.00 e^{-97}	93.57
DN31858_c0_g1	*ILP4*	Insulin-like peptide 4 protein [*Chrysopa pallens*]	QOY58108.1	1.00 e^{-68}	81.16
DN3112_c0_g1	*InR1*	Insulin-like peptide receptor 1 [*Chrysopa pallens*]	AVK43098.1	0	79.85
DN1172_c3_g2	*InR2*	Insulin-like peptide receptor 2 [*Chrysopa pallens*]	AVK43099.1	0	91.87
DN3135_c0_g1	*IDE*	Insulin-degrading enzyme [*Anoplophora glabripennis*]	XP_018580177.1	0	63.28
DN2538_c3_g1	*mTOR*	Serine/threonine-protein kinase mTOR isoform X2 [*Cryptotermes secundus*]	XP_023715968.1	0	66.33
DN2866_c0_g1	*S6K*	Ribosomal protein S6 kinase beta-1 isoform X1 [*Cryptotermes secundus*]	XP_023714623.1	0	64.02
DN732_c0_g1	*Reb*	GTP-binding protein Rheb homolog [*Cephus cinctus*]	XP_015600975.1	1.00 e^{-113}	85.16
DN28_c0_g2	*FoxO*	FoxO [*Chrysopa pallens*]	QBC41003.1	0	96.74
DN4060_c0_g1	*AMPK*	5′-AMP-activated protein kinase subunit beta-1 [*Photinus pyralis*]	XP_031339135.1	1.00 e^{-158}	80.66
DN2860_c1_g1	*Akt*	Akt [*Chrysopa pallens*]	QBC41002.1	0	99.45
DN2244_c0_g4	*Raptor*	mTOR regulatory-associated protein [*Chrysopa pallens*]	QBC41004.1	0	97.92
DN2877_c4_g1	*ERK*	Mitogen-activated protein kinase [*Chrysopa pallens*]	QFP92286.1	0	100
DN896_c2_g1	*Pten*	Phosphatidylinositol 3,4,5-trisphosphate 3-phosphatase and dual-specificity protein phosphatase PTEN isoform X3 [*Cryptotermes secundus*]	XP_023719842.1	0	59.27
DN3984_c0_g3	*Pi3K*	Phosphatidylinositol-4-phosphate 3-kinase C2 domain-containing beta polypeptide [*Harpegnathos saltator*]	EFN80176.1	0	56.63
DN3016_c3_g1	*lnK*	SH2B adapter protein 1 isoform X2 [*Zootermopsis nevadensis*]	XP_021939259.1	0	60.31
DN1293_c0_g1	*LPIN*	Phosphatidate phosphatase LPIN2 [*Onthophagus taurus*]	XP_022912893.1	0	54.63
Marker Genes					
DN920_c4_g1	*Vg*	Vitellogenin [*Chrysoperla nipponensis*]	QQO58845.1	0	100
DN2198_c1_g1	*VgR*	Vitellogenin receptor [*Chrysoperla nipponensis*]	QQK84939.1	0	99.89

Abbreviations: ECD, ecdysterone; GTP, guanosine triphosphate; JH, juvenile hormone; mTOR, mammalian target of rapamycin; TOR, target of rapamycin.

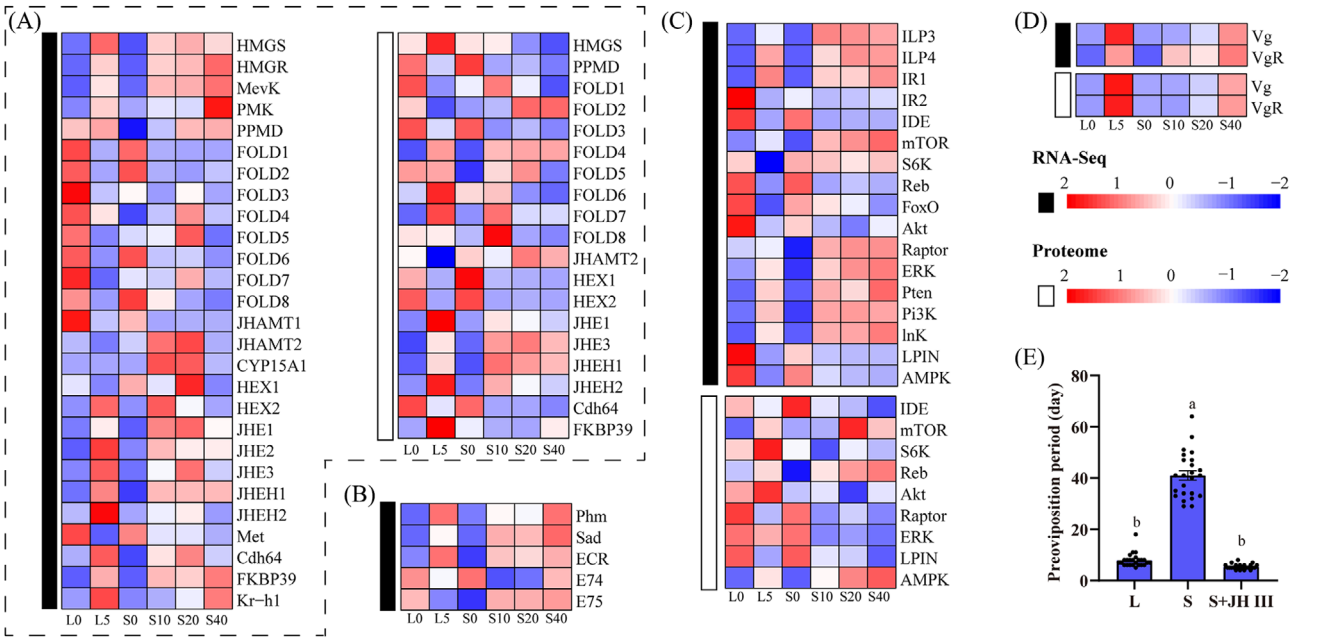

FIGURE 6. Heat maps of insect hormone genes and proteins of *Chrysoperla nipponensis* female during adult reproductive diapause. (A) Juvenile hormone (JH) related genes. (B) Molting hormone related genes. (C) Genes involved in insulin/TOR pathway. (D) Marker genes. (E) Effects of JH III on pre-oviposition period of diapausing female adults. Data are presented as means of three independent samples.

cluster 1 were highly enriched in the metabolic pathway, carbon metabolism, and citrate cycle (TCA cycle; Figures 4B and S3). Genes in clusters 2 and 6 were involved in fatty acid metabolism, insect hormone and carbohydrate utilization (Figures 4B and S3).

3.3 Analysis of differential expressions of genes and proteins

The differential expressions of genes and proteins are given in Table 1. Multiple comparisons of different treatments are also provided in Tables S2 and S3. S0 had fewer than 100 differentially expressed genes and proteins compared with L0, whereas L5 had significantly different expression profiles for more than 5000 genes and 1803 proteins (Table 1). Around 2000 genes showed different expression levels in S10, S20, and S40 compared with S0 (Table 1).

The majority of circadian genes could be found only at the transcript level (Table 2 and Figure 5A). Only *CRY1*, a blue-light photoreceptor, was detected at both the transcript and protein levels (Table 2 and Figure 5A). The expression pattern of *CLK* was similar to *VgR* (Figure 5). *PER*, *TIM* and *CYC* showed the highest expression levels in L0, whereas *CRY1* showed the highest transcript and protein levels in S10 (Figure 5A). In diapause female adults of *C. nipponensis*, *CRY1* was primarily expressed at the transcript level (Figure 5A). *TIM* was considerably downregulated in S0, S10 and S20 compared with L0 and L5 (Figure 5A). However, its expression increased in S40 (Figure 5A). Expression patterns of *Vg* and *VgR* differed at the transcript level, but were similar at the protein level (Figure 5B).

The JH synthesis genes *JHAMT2* and *CYP15A1* were highly expressed in S10 and S20, whereas JHAMT2 protein had a higher abundance in S0, S20 and S40 (Table 3 and Figure 6A). Expression levels of *HMGS*, *HMGR*, and *MevK* were higher in L5, S10, S20 and S40 than in S0 and L0 (Figure 6A). Genes of *FOLD* showed relatively higher expression in L0 at the transcript level, but there were no clear expression patterns in the proteome (Figure 6A). The majority of JH degradation-related genes were highly expressed in L5, S10, S20, and S40 at both the transcriptomic and proteomic levels (Figure 6A). In newly emerged adults (S0 and L0), JH receptor *Met* expression was higher, and then subsequently decreased (Figure 6A). However, *FKBP39*, which participated in JH reception and cell metabolism, showed a reversed pattern of expression to *Met* (Figure 6A).[45] Expression of ecdysone-related genes was consistent with JH degradation-related genes (Figure 6B). Similarly, *ILP3*, *ILP4*, *IR1*, *ERK*, *Pten*, *Pi3K*, *lnK* and *VgR* were highly expressed in L5, S10, S20 and S40 (Figure 6C,D). *PMK*, *Kr-h1*, *Phm* and *Vg* were only upregulated in L5 and S40 (Figure 6). Interestingly, at the transcript level, *mTOR* was predominately expressed in diapause female adults although it was upregulated at the protein level in only L5 and S40 (Figure 6C). Topical application of JH III rescued the reproductive arrest (df = 2; $F = 321.7$; $p < 0.001$) of *C. nipponensis* under a short photoperiod, and no impairment in fecundity was observed (df = 2; $F = 22.48$; $p < 0.001$) in rescued diapause female adults (Figures 6E and S4). The qPCR results for *JHAMT2* (df = 5; $F = 55.16$; $p < 0.001$), *Kr-h1* (df = 5; $F = 166.6$; $p < 0.001$), *ILP3* (df = 5; $F = 154.9$; $p < 0.001$), *ILP4* (df = 5; $F = 48.61$; $p < 0.001$), *IR1* (df = 5; $F = 142.5$; $p < 0.001$), *Vg* (df = 5; $F = 177.2$; $p < 0.001$) and *VgR* (df = 5; $F = 38.40$; $p < 0.001$) showed expression profiles similar to the transcriptomic results (Figure S5).

Only two of six putative fatty acid synthesis genes were detected at both the transcript and protein levels (Table 4 and Figure 7). When exposed to a short photoperiod, expression of *ACC* was increased and was also higher in L5 than in L0 at the protein level (Figure 7). *β*-Oxidation, lipid transport and storage genes displayed similar expression profiles at the transcript and protein levels (Figure 7). At the protein level, expression of *CPT-3*, *ACD-1*, *ACD-2*, *ACD-4*, ACD-6, *LSD1*, *HCDH-2*, and *BK-2* was upregulated during reproductive diapause, whereas *CPT-1*, *CPT-2*, *ACD-3* and *ACD-5* showed higher expression in L0 and S0 than in L5, S10, S20 and S40 (Figure 7). At the transcript level, expression of lipase

TABLE 4. Putative fat metabolism genes in *Chrysoperla nipponensis*

Gene IDs	Gene name	Best blast	Accession	e-value	Percent identity
Fatty acid synthase					
DN7710_c0_g1	FAS1	Fatty acid synthase-like, partial [*Glossina fuscipes*]	XP_037899273.1	5.00 e^{-131}	55.14
DN187_c1_g3	FAS2	Fatty acid synthase-like [*Zootermopsis nevadensis*]	XP_021921613.1	2.00 e^{-114}	44.47
DN6771_c0_g1	FAS3	Fatty acid synthase [*Diaphorina citri*]	XP_026678910.1	1.00 e^{-131}	40.70
DN3824_c1_g1	FAS4	Fatty acid synthase-like [*Diaphorina citri*]	XP_017299284.2	2.00 e^{-120}	52.34
DN6253_c0_g1	FAS5	Fatty acid synthase [*Aphis craccivora*]	KAF0747563.1	7.00 e e^{-162}	58.27
Acetyl-CoA carboxylase					
DN291_c1_g1	ACC	PREDICTED: acetyl-CoA carboxylase isoform X4 [*Tribolium castaneum*]	XP_008194742.1	0	78.04
β-Oxidation					
Acetyl-CoA synthetase					
DN361_c0_g1	ACS1	Long-chain-fatty-acid--CoA ligase ACSBG2 [*Onthophagus taurus*]	XP_022915628.1	0	60.84
DN1139_c4_g1	ACS2	PREDICTED: long-chain-fatty-acid--CoA ligase 4 isoform X7 [*Tribolium castaneum*]	XP_008193865.1	0	62.84
Carnitine palmitoyl transferases I, II					
DN2137_c4_g1	CPT1	Carnitine *O*-palmitoyltransferase 2, mitochondrial-like [*Aedes albopictus*]	XP_019535807.2	0	55.75
DN229_c0_g1	CPT2	Carnitine *O*-palmitoyltransferase 1, liver isoform-like isoform X1 [*Onthophagus taurus*]	XP_008191464.1	0	79.24
DN3408_c0_g1	CPT3	Carnitine *O*-acetyltransferase isoform X2 [*Diabrotica virgifera virgifera*]	XP_028131132.1	8.00 e^{-118}	52.29
Acyl-CoA dehydrogenase					
DN2949_c0_g1	ACD1	Short-chain specific acyl-CoA dehydrogenase, mitochondrial-like [*Leptinotarsa decemlineata*]	XP_023017723.1	0	74.93
DN23094_c0_g1	ACD2	PREDICTED: very long-chain specific acyl-CoA dehydrogenase, mitochondrial [*Tribolium castaneum*]	XP_966406.1	0	75.00
DN3456_c0_g2	ACD3	Short/branched chain specific acyl-CoA dehydrogenase, mitochondrial [*Diabrotica virgifera virgifera*]	XP_028140001.1	0	70.05
DN712_c2_g1	ACD4	PREDICTED: short-chain specific acyl-CoA dehydrogenase, mitochondrial [*Tribolium castaneum*]	XP_972925.2	0	81.66
DN1476_c2_g1	ACD5	Isovaleryl-CoA dehydrogenase, mitochondrial [*Onthophagus taurus*]	XP_022901928.1	0	75.18
DN40879_c0_g2	ACD6	Probable enoyl-CoA hydratase, mitochondrial [*Trichogramma pretiosum*]	XP_014235067.1	5.00 e^{-82}	77.63
Hydroxyacyl-CoA dehydrogenase					
DN12039_c0_g1	HCDH1	3-Hydroxyacyl-CoA dehydrogenase type-2 [*Hermetia illucens*]	XP_037903042.1	5.00 e^{-115}	60.97
DN55626_c0_g3	HCDH2	PREDICTED: hydroxyacyl-coenzyme A dehydrogenase, mitochondrial-like [*Nicrophorus vespilloides*]	XP_017777518.1	1.00 e^{-172}	75.81
DN3983_c0_g2	HCDH3	3-Hydroxyisobutyryl-CoA hydrolase, mitochondrial isoform X1 [*Onthophagus taurus*]	XP_022906940.1	6.00 e^{-117}	49.58
β-Ketoacyl					
DN15442_c0_g1	BK1	3-Ketoacyl-CoA thiolase B, peroxisomal [*Clavispora lusitaniae*]	KAF7581011.1	0	85.58
DN8531_c10_g1	BK2	3-Ketoacyl-CoA thiolase, mitochondrial-like [*Leptinotarsa decemlineata*]	XP_023015250.1	8.00 e^{-155}	66.99
Lipid transport					
DN3229_c0_g2	FATP	Long-chain fatty acid transport protein 4-like isoform X1 [*Athalia rosae*]	XP_012262719.1	0	68.48
Lipid storage					
DN1627_c2_g2	LSD1	Lipid storage droplets surface-binding protein 1 isoform X2 [*Chrysoperla carnea*]	XP_044727334.1	0	99.79
DN4716_c0_g2	LSD2	Lipid storage droplets surface-binding protein 2 isoform X1 [*Chrysoperla carnea*]	XP_044734514.1	2.00 e^{-140}	99.48
Lipolysis					
DN2072_c0_g2	Lipase	Hormone-sensitive lipase isoform X2 [*Zootermopsis nevadensis*]	XP_021913536.1	0	44.06
Polyunsaturated fatty acid synthesis					
DN33923_c0_g1	FAD1	Acyl-CoA Delta(11) desaturase [*Frankliniella occidentalis*]	XP_026284985.1	9.00 e^{-119}	49.39
DN1803_c0_g1	FAD2	Acyl-CoA Delta(11) desaturase [*Anoplophora glabripennis*]	XP_018579074.1	3.00 e^{-137}	53.91
DN9776_c0_g2	FAD3	Acyl-CoA Delta(11) desaturase [*Cephus cinctus*]	XP_015589801.1	2.00 e^{-172}	65.52

TABLE 4. Continued

Gene IDs	Gene name	Best blast	Accession	e-value	Percent identity
DN1695_c0_g1	FAD4	Acyl-CoA Delta(11) desaturase [*Trichogramma pretiosum*]	XP_014227952.1	9.00 e^{-125}	54.18
DN1942_c0_g1	FAD5	Acyl-CoA Delta(11) desaturase [*Acyrthosiphon pisum*]	XP_001943917.1	3.00 e^{-88}	58.25
DN2362_c0_g3	FAD6	Acyl-CoA Delta(11) desaturase [*Zootermopsis nevadensis*]	KDR08705.1	0	71.39
DN1731_c0_g2	FAD7	Acyl-CoA Delta(11) desaturase [*Blattella germanica*]	PSN55622.1	4.00 e^{-178}	58.64
DN29236_c0_g2	FAD8	PREDICTED: acyl-CoA Delta(11) desaturase-like [*Neodiprion lecontei*]	XP_015512919.1	1.00 e^{-152}	64.72
DN1358_c0_g1	FAD9	PREDICTED: acyl-CoA Delta(11) desaturase-like [*Dendroctonus ponderosae*]	XP_019759806.1	5.00 e^{-54}	56.58
DN954_c0_g2	FAD10	Sphingolipid delta(4)-desaturase DES1 [*Athalia rosae*]	XP_012255918.1	0	81.21%
Nuclear hormone receptor					
DN6105_c0_g1	NHR1	Nuclear hormone receptor FTZ-F1 beta [*Photinus pyralis*]	XP_031332667.1	0	64.59
DN1241_c0_g1	NHR2	Nuclear hormone receptor FTZ-F1-like isoform X2 [*Photinus pyralis*]	XP_031356518.1	0	62.60

in newly emerged adults (L0 and S0) was higher than in L5, S10, S20 and S40, and was higher during reproductive diapause (Figure 7). *ACC* (df = 5; $F = 22.74$; $p < 0.001$), *ACD6* (df = 5; $F = 61.52$; $p < 0.001$) and *FAD6* (df = 5; $F = 241.8$; $p < 0.001$) showed the highest abundance in S40, whereas *CPT3* (df = 5; $F = 10.14$; $p < 0.001$), *HCDH3* (df = 5; $F = 26.64$; $p < 0.001$), *LSD1* (df = 5; $F = 63.43$; $p < 0.001$) and *LSD2* (df = 5; $F = 37.21$; $p < 0.001$) were most abundant in S10 (Figure S5). Gene expression patterns from qPCR results were consistent with their expression levels in the transcriptome (Figures 7 and S5).

Based on the expression profile of genes and proteins related to lipid metabolism, L0 and S0 clustered beside the proteomic results in glycerophospholipid metabolism (Figure S6). More genes were significantly higher in L5, S10, S20, and S40 (Figure S6). At the protein levels, the abundance of glycerophospholipid-related proteins was higher in S10 S20, and S40 than in L0, S0 and L5 (Figure S6). Only a small number of differential genes and proteins were found in sphingolipid metabolism (Figure S6).

At the transcript level, the expression of glucose-6-phosphate isomerase genes was significantly higher in diapause female adults than in non-diapause female adults. By contrast, two of these genes were predominately expressed in L5 at the protein level (Figure 8A). Compared with other treatments, L5 exhibited significantly higher levels of the genes for fructose-bisphosphate aldolase, glyceraldehyde 3-phosphate dehydrogenase, triosephosphate isomerase and enolase (Figure 8A). Interestingly, the major genes involved in TCA cycles showed considerably greater protein abundance in S10, S20, and S40 compared with L0, L5, and S0 (Figure 8B). However, no clear expression patterns were observed at the transcript level (Figure 8B). The hexokinase, triosephosphate isomerase, phosphoglucomutase, dihydrolipoamide dehydrogenase, 2-oxoglutarate dehydrogenase E1 component and isocitrate dehydrogenase showed significantly higher expression levels in L5 and S20 (Figure 8).

4 DISCUSSION

Generally, insects increase the accumulation of energy reserves during the diapause preparation stage and depress metabolism during diapause.[1,2] In this study, we found greater weight gain in field overwintering populations and short photoperiod-induced diapause female adults of *C. nipponensis*. Similarly, pre-diapause females of *Colaphellus bowringi* and diapause pupae of both female and male *Hyphantria cunea* have higher dry weights.[7,46] Previous studies demonstrated that lipids are one of the most important energy reserves in diapause insects.[1,2,8] Our results showed obvious accumulations of total lipid and TAG content in female adults of *C. nipponensis* during overwintering and in short photoperiod-induced diapause female adults. In *Colaphellus bowringi* and *H. cunea*, diapause insects had higher lipid accumulations and TAG content than non-diapause insects.[46,47] The carbohydrate, lipid, and TAG contents in pre-diapause female adults of *H. axyridis* are significantly higher than in pre-productive female adults. By contrast, pre-diapause males only accumulate more carbohydrates.[9,16] *Ips typographus* had reduced post-diapause fitness and higher mortality when nutritional reserves were low.[48] These findings demonstrated that diapause female adults of *C. nipponensis* hold more energy resources and inhibit their metabolism to successfully withstand the winter.

Our previous studies showed that a short photoperiod induces reproductive diapause in *C. nipponensis*.[38,39] The circadian genes

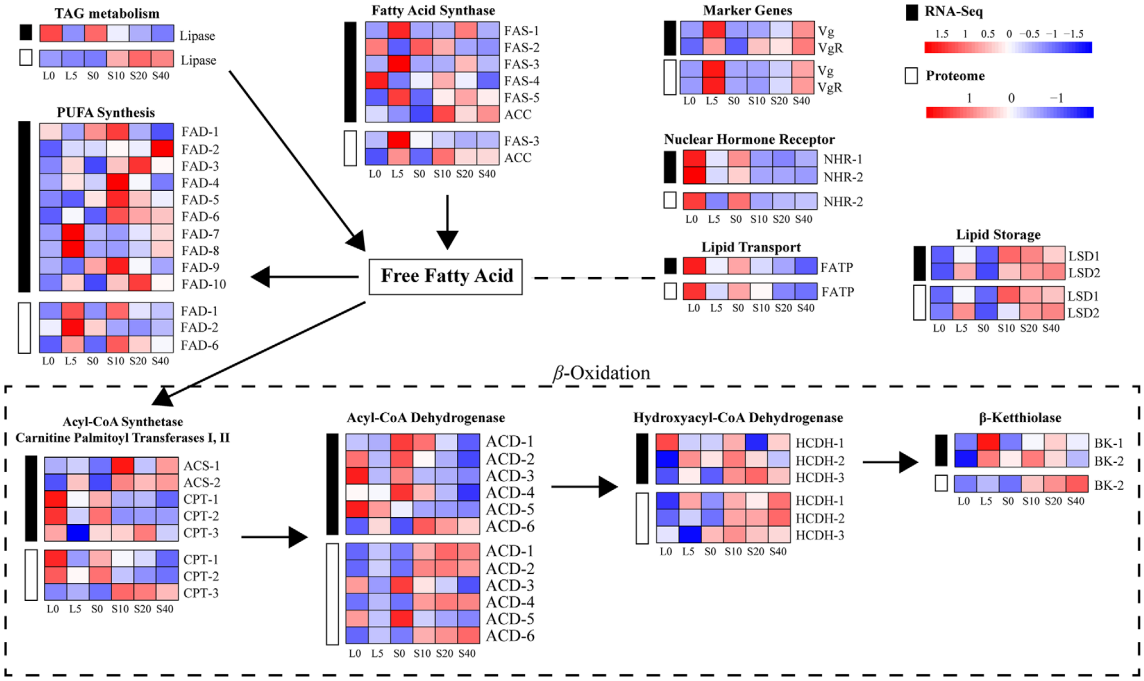

FIGURE 7. Putative *Chrysoperla nipponensis* fatty acid metabolism pathway. Data are presented as means of three independent samples.

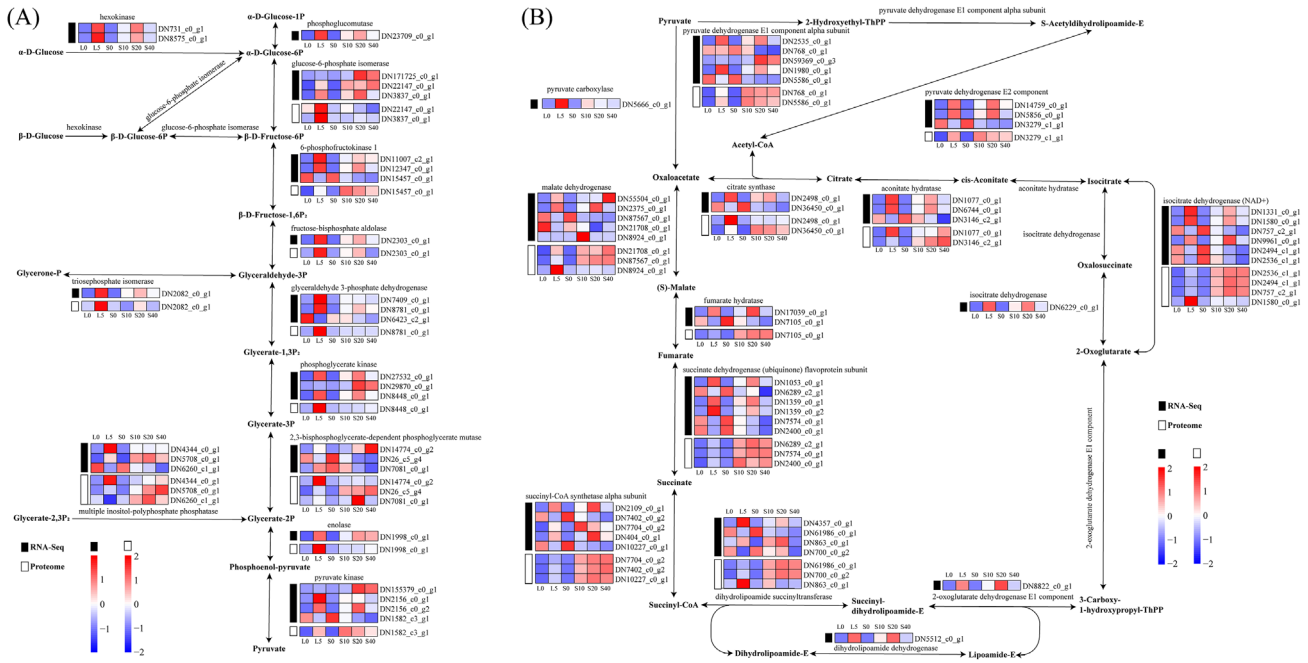

FIGURE 8. Heat map of genes and proteins involved in glycolysis (A) and citrate cycle (TCA cycle) (B). Data are presented as means of three independent samples.

are involved in photoperiod sensing.[49] Transcriptome and proteome results showed that the expression pattern of *CLK* was similar to that of *VgR*, and the *TIM* expression pattern was more consistent with expression of *Vg*. In *Riptortus pedestris*, injection with CLK double-strand RNA (dsRNA) did not influence on the diapause female, although it caused ovarian development arrest in non-diapause females.[50] Recently, Zhu et al. reported that knockdown of *TIM* in *Colaphellus bowringi* did not affect diapause-destined females but impaired lipid accumulation during the diapause preparation phase.[47] By contrast, *TIM* dsRNA-injection averted diapause in *Culex pipiens*.[51] Our finding of *TIM* and *CLK* expression patterns suggest that they might be

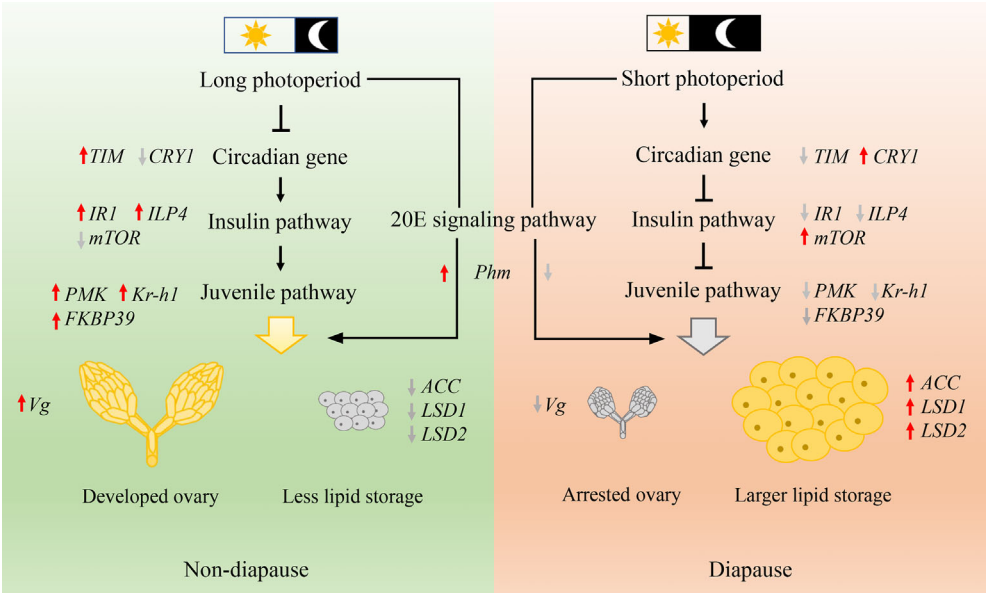

FIGURE 9. Potential model explaining how photoperiod regulates reproduction and diapause in *Chryaoperla nipponensis*. Under the short photoperiod, *TIM* expression is downregulated, whereas *CRY1* is upregulated. These photoperiodic response genes inhibit the expression of key genes in the insulin pathway such as *IR1* and *ILP4*, but stimulate *mTOR* expression. Suppression of the insulin signal subsequently blocks juvenile hormoe (JH; *PMK*) and 20-hydroxyecdysone (20E; *Phm*) synthesis, thereby results in lower expression *Kr-h1*, which finally stimulates *ACC*, *LSD1* and *LSD2* expression for lipid accumulation and inhibits the expression of Vg leading to ovarian dormancy. However, under the long photoperiod condition, insulin, JH and 20E are synthesized normally, thereby triggering ovarian development and lipid utilization.

important in diapause induction and maintenance in *C. nipponensis*.

The insulin pathway is crucial to initiating insect diapause by regulating ovarian development and nutritional metabolism.[26,27] Our transcriptome and proteome results showed that the expression patterns of *ILP4*, *IR1*, *ERK*, *Pten*, *Pi3K*, and *lnK* were similar to that of *VgR*, and *ILP3*, *mTOR* and Raptor were predominately expressed in diapause females of *C. nipponensis*. However, at the protein level, only *mTOR* and *AMPK* showed expression patterns similar to *Vg* and *VgR*. Triple deletion of *ILP2*, *-3* and *-5* led to strong induction of diapause in *Drosophila melanogaster*, whereas their overexpression rescued ovarian dormancy.[52] Han et al. reported that inhibited expression of *IR2* resulted in depression of ovarian development, a typical diapause phenotype in reproductive diapause insects.[31] Depletion of *InR* and *ILP-1* prevented ovarian maturation in non-diapause female adults of *Culex pipiens*.[27,30] Application of the JH analog methoprene rescued ovarian development in *dsInR*-injected *Culex pipiens*.[27] RNAi knockdown of *IR* delayed ovarian development and resulted in a lower JH titer.[53] Similarly, mutation of *IR* reduced JH synthesis in *D. melanogaster*.[54] These findings suggested that the insulin pathway is involved in the insect diapause process by altering the JH synthesis.

Numerous studies have shown that insect hormones such as JH and ecdysone are essential for insect diapause induction, maintenance and termination.[1,26] Our combined transcriptomic and proteomic analyses showed that expression of *HMGS*, *HMGR*, *MevK*, *JHEH1*, *FKBP39*, and *ECR* were consistent with the expression of *VgR*. By contrast, only *PMK*, *Kr-h1*, and *Phm* showed similar expression profiles to *Vg* (Figure 6). *mTOR* was predominately expressed in diapause females at the transcript level, whereas its expression patterns at the protein level were similar to those of *Vg* (Figure 6). Topical application of JH III rescued reproductive arrest under a short photoperiod (Figure 6). In *Colaphellus bowringi*, genes involved in JH biosynthesis and degradation were suppressed under diapause-inducing conditions.[47,55,56] Knockdown of *HMGR* and *JHAMT* significantly arrested female reproduction and caused lipid accumulation in the fat body.[56] Similarly, silencing of *JHAMT* in *L. decemlineata*, *H. axyridis*, *S. furcifera* and *B. germanica* also induced ovarian arrest.[16,18–20] Expression of *Kr-h1* in *H. axyridis*, *Colaphellus bowringi* and *G. daurica* showed lower transcript levels in diapause female adults than in non-diapause female adults.[14,16,17,21] Injection of *dsKr-h1* in *H. axyridis* and *Colaphellus bowringi* resulted in ovarian arrest, higher expression of lipogenesis genes, and nutrient accumulation.[16,17,21,23] Thus, we speculated that differentially expressed JH-related genes, especially *Kr-h1*, *PMK* and *HMGR*, between non-diapause and diapause female adults of *C. nipponensis* should be involved in the maintenance of diapause. Recently, Guo et al. found that non-diapause female adults of *Colaphellus bowringi* had a significantly higher titer of 20-hydroxyecdysone (20E) and exogenous 20E could induce ovary development in diapause female adults.[57] More interestingly, exogenous 20E treatment significantly increased the biosynthesis of JH and upregulated the expression of JH-related genes.[57] Knockdown of *ECR* in non-diapause female adults had a reproductive defect, and juvenile hormone analog (JHA) application can rescue this defect.[57] Consistent with our results, lower expression of *Phm* was observed during diapause in *Colaphellus bowringi*, *Chymomyza costata*, and *Mamestra brassicae*.[57–59] These results indicated that a short photoperiod might induce reproductive diapause in *C. nipponensis* by altering the expression of genes in the JH and 20E signaling pathways.

As noted earlier, lipid accumulation and inhibition of lipid metabolism were found in diapause female adults of *C. nipponensis*. Our transcriptome and proteome results showed that *ACC*, which converts sugar to fat, and *LSD1* and *LSD2*, which are involved in lipid accumulation, showed increased expression in diapause females of *C. nipponensis* (Figures 6 and S4).[2,60–62]

Similarly, expression of *ACC* was higher in diapause female adults of *Coccinella septempunctata* than in non-diapause female adults.[61] Knockdown of *ACC* led to decreased lipid content in diapause female adults of *C. septempunctata*.[61] *LSD2* transcript levels were significantly higher in diapause females of *Aedes albopictus* and *L. decemlineata* than in non-diapause females.[60,63] *LSD2* depletion decreased the lipid content in *L. decemlineata*.[60] In *Lissorhoptrus oryzophilus*, *LSD1* showed a higher expression level in overwintering female adults, whereas *LSD2* showed higher expression in summer female adults.[64] Consistent with these previous studies, our results revealed that *ACC*, *LSD1*, and *LSD2* might be key genes involved in lipid accumulation and storage in *C. nipponensis* during reproductive diapause.

5 CONCLUSION

In this study, we quantitively analyzed the weight, lipid and TAG content in female adults of *C. nipponensis* during overwintering and reproductive diapause. We found that diapause female adults of *C. nipponensis* retain more energy resources and inhibit metabolism of these resources to successfully overwinter (Figure 9). In addition, we also presented a large-scale investigation of global gene and protein expression changes during reproductive diapause of female adults using transcriptome and proteome analysis. The results showed that *TIM* and *CRY1* might be involved in photoperiod sensing (Figure 9). Moreover, the JH, 20E and insulin signaling pathway genes, especially *PMK*, *FKBP39*, *Kr-h1*, *Phm*, *IR1*, *ILP4*, and *mTOR*, might be involved in the induction and regulation of reproductive diapause in *C. nipponensis* (Figure 9). *ACC*, *LSD1*, and *LSD2* might be the key genes linked with lipid accumulation and storage (Figure 9). Further functional studies on these candidate genes are required to understand the molecular mechanisms regulating *C. nipponensis* reproductive diapause. Our rescue experiment of reproductive arrest by topical application of JH III suggested that *C. nipponensis* could be a promising commercial biological agent by combining mass-rearing and mass storage under a short photoperiod in the factory and rescue with JH III before release in the greenhouse or field. Overall, the results of this study provided basic information toward understanding reproductive diapause and facilitating the mass production and storage of *C. nipponensis*.

ACKNOWLEDGMENTS

This work was supported by the National Science Foundation of Shandong Province (ZR2020MC047 and ZR2022MC179), the National Natural Science Foundation of China (315015904), the National Key Research and Development Program of China (2017YFD0201000) and Hebei Natural Science Foundation (C2022201042). The authors would like to thank to Yi-Heng Li (Jingjie PTM BioLabs, Hangzhou, Zhejiang, China) for his help in raw data submission and all members in the Laboratory of Insect Eco-Physiology, Shandong Agricultural University for their assistances in plant and insect rearing.

CONFLICTS OF INTEREST

The authors declare that the research was conducted in the absence of any commercial or financial relationships that could be construed as a potential conflict of interest.

DATA AVAILABILITY STATEMENT

The data that support the findings of this study are available in NCBI at https://www.ncbi.nlm.nih.gov/, reference number PRJNA788306. These data were derived from the following resources available in the public domain: - RNA-seq of C. nipponensis female adults during diapause, https://dataview.ncbi.nlm.nih.gov/object/PRJNA788306.

SUPPORTING INFORMATION

Supporting information may be found in the online version of this article.

REFERENCES

1 Hahn DA and Denlinger DL, Energetics of insect diapause. *Annu Rev Entomol* **56**:103–121 (2011).
2 Denlinger DL and Armbruster PA, Chapter eleven-Molecular physiology of mosquito diapause, in *Advances in Insect Physiology*, Vol. **51**, ed. by Raikhel AS. MA, Chapter 11, Academic Press, Cambridge, pp. 329–361 (2016).
3 Wang J, Fan H, Xiong KC and Liu YH, Transcriptomic and metabolomic profiles of Chinese citrus fly, *Bactrocera minax* (Diptera: Tephritidae), along with pupal development provide insight into diapause program. *PLoS One* **12**:e0181033 (2017).
4 Yang MY, Wang ZC, Wang R, Zhang XM, Li MY, Xin JJ *et al*., Transcriptomic and proteomic analyses of the mechanisms of overwintering diapause in soybean pod borer (*Leguminivora glycinivorella*). *Pest Manage Sci* **76**:4248–4257 (2020).
5 Hou YY, Xu LZ, Wu Y, Wang P, Shi JJ and Zhai BP, Geographic variation of diapause and sensitive stages of photoperiodic response in *Laodelphax striatellus* Fallen (Hemiptera: Delphacidae). *J Insect Sci* **16**: 13 (2016).
6 Xue FS, Spieth HR, Li AQ and Ai H, The role of photoperiod and temperature in determination of summer and winter diapause in the cabbage beetle, *Colaphellus bowringi* (coleoptera: Chrysomelidae). *J Insect Physiol* **48**:279–286 (2002).
7 Tan QQ, Feng L, Liu W, Zhu L, Lei CL and Wang XP, Differences in the pre-diapause and pre-oviposition accumulation of critical nutrients in adult females of the beetle *Colaphellus bowringi*. *Entomol Exp Appl* **160**:117–125 (2016).
8 Sim C and Denlinger DL, Transcription profiling and regulation of fat metabolism genes in diapausing adults of the mosquito *Culex pipiens*. *Physiol Genomics* **39**:202–209 (2009).
9 Gao Q, Wei BX, Liu W, Wang JL, Zhou XM and Wang XP, Differences in the development of internal reproductive organs, feeding amount and nutrient storage between pre-diapause and pre-reproductive *Harmonia axyridis* adults. *Insects* **10**:243 (2019).
10 Li K, Jia QQ and Li S, Juvenile hormone signaling-a mini review. *Insect Sci* **26**:600–606 (2019).
11 Jindra M, Belles X and Shinoda T, Molecular basis of juvenile hormone signaling. *Curr Opin Insect Sci* **11**:39–46 (2015).
12 Jindra M, Palli SR and Riddiford LM, The juvenile hormone signaling pathway in insect development. *Annu Rev Entomol* **58**:181–204 (2013).
13 Chen H, Wu GA, Zhou H, Dai XY, Steeghs NWF, Dong XL *et al*., Hormonal regulation of reproductive diapause that occurs in the year-round mass rearing of *Bombus terrestris* queens. *J Proteome Res* **20**:2240–2250 (2021).
14 Gao Q, Li B, Wei BX, Liu W, Wang P, Wang JL *et al*., Juvenile hormone regulates photoperiod-mediated male reproductive diapause via the methoprene-tolerant gene in the ladybeetle *Harmonia axyridis*. *Insect Sci* **0**:1–12 (2021).
15 Readio J, Chen MH and Meola R, Juvenile hormone biosynthesis in diapausing and nondiapausing *Culex pipiens* (Diptera: Culicidae). *J Med Entomol* **36**:355–360 (1999).
16 Gao Q, Li B, Tian Z, De Loof A, Wang JL, Wang XP *et al*., Key role of juvenile hormone in controlling reproductive diapause in females of the Asian lady beetle *Harmonia axyridis*. *Pest Manage Sci* **78**:193–204 (2021).
17 Liu W, Li Y, Zhu L, Zhu F, Lei CL and Wang XP, Juvenile hormone facilitates the antagonism between adult reproduction and diapause

through the *methoprene-tolerant* gene in the female *Colaphellus bowringi*. *Insect Biochem Mol Biol* **74**:50–60 (2016).
18 Zhou C, Yang XB, Yang H, Gong MF, Long GY and Jin DC, Role of *SfJHAMT* and *SfFAMeT* in the reproductive regulation of *Sogatella furcifera* and its expression under insecticide stress. *Pestic Biochem Physiol* **173**:104779 (2021).
19 Fu KY, Li Q, Zhou LT, Meng QW, Lu FG, Guo WC *et al*., Knockdown of juvenile hormone acid methyl transferase severely affects the performance of *Leptinotarsa decemlineata* (Say) larvae and adults. *Pest Manage Sci* **72**:1231–1241 (2016).
20 Dominguez CV and Maestro JL, Expression of juvenile hormone acid O-methyltransferase and juvenile hormone synthesis in *Blattella germanica*. *Insect Sci* **25**:787–796 (2018).
21 Guo S, Wu QW, Tian Z, Zhu L, King-Jones K, Zhu F *et al*., Krüppel homolog 1 regulates photoperiodic reproductive plasticity in the cabbage beetle *Colaphellus bowringi*. *Insect Biochem Mol Biol* **134**:103582 (2021).
22 Smykal V, Bajgar A, Provaznik J, Fexova S, Buricova M, Takaki K *et al*., Juvenile hormone signaling during reproduction and development of the linden bug, Pyrrhocoris apterus. *Insect Biochem Mol Biol* **45**: 69–76 (2014).
23 Ma HY, Li YY, Li L, Tan Y and Pang BP, Juvenile hormone regulates the reproductive diapause through Methoprene-tolerant gene in *Galeruca daurica*. *Insect Mol Biol* **30**:446–458 (2021).
24 Mao YW, Li Y, Gao H and Lin XD, The direct interaction between E93 and Kr-h1 mediated their antagonistic effect on ovary development of the brown planthopper. *Int J Mol Sci* **20**:2431 (2019).
25 Song JS, Wu ZX, Wang SM, Deng S and Zhou ST, Krüppel-homolog 1 mediates juvenile hormone action to promote vitellogenesis and oocyte maturation in the migratory locust. *Insect Biochem Mol Biol* **52**:94–101 (2014).
26 Sim C and Denlinger DL, Insulin signaling and the regulation of insect diapause. *Front Physiol* **4**:189 (2013).
27 Sim C and Denlinger DL, Insulin signaling and FOXO regulate the overwintering diapause of the mosquito *Culex pipiens*. *Proc Natl Acad Sci U S A* **105**:6777–6781 (2008).
28 Li YN, Ren XB, Liu ZC, Ye B, Zhao ZJ, Fan Q *et al*., Insulin-like peptide and FoxO mediate the trehalose catabolism enhancement during the diapause termination period in the Chinese oak silkworm (*Antheraea pernyi*). *Insects* **12**:784 (2021).
29 Arpagus M, Vertebrate insulin induces diapause termination in *Pieris brassicae* pupae. *Rouxs Arch Dev Biol* **196**:527–530 (1987).
30 Sim C and Denlinger DL, A shut-down in expression of an insulin-like peptide, ILP-1, halts ovarian maturation during the overwintering diapause of the mosquito *Culex pipiens*. *Insect Mol Biol* **18**:325–332 (2009).
31 Han BF, Zhang TT, Feng YJ, Liu XP, Zhang LS, Chen HY *et al*., Two insulin receptors coordinate oogenesis and oviposition via two pathways in the green lacewing, Chrysopa pallens. *J Insect Physiol* **123**:104049 (2020).
32 Yin ZJ, Dong XL, Kang K, Chen H, Dai XY, Wu GA *et al*., FoxO transcription factor regulate hormone mediated signaling on nymphal diapause. *Front Physiol* **9**:1654 (2018).
33 Chen ZZ, Liu LY, Liu SY, Cheng LY, Wang XH and Xu YY, Response of *Chrysoperla nipponensis* (Okamoto) (Neuroptera: Chrysopidae) under long and short photoperiods. *J Insect Sci* **17**:35 (2017).
34 Montoya-Alvarez AF, Ito K, Nakahira K and Arakawa R, Functional response of *Chrysoperla nipponensis* and *C. carnea* (Neuroptera: Chrysopidae) to the cotton aphid *Aphis gossypii* glover (Homoptera: Aphididae) under laboratory conditions. *Appl Entomol Zool* **45**:201–206 (2010).
35 Huang HY, Liu YN, Qi YF, Xu YY and Chen ZZ, Predatory responses of *Chrysoperla sinica* (Tjeder) larvae to *Spodoptera frugiperda* (J. E. Smith) eggs and larvae. *Chinese. J Appl Entomol* **57**:1333–1340 (2020).
36 Tang TC, Zhang Y, Li CJ, Cao XR, Chen ZZ and Xu YY, Predatory responses of *Chrysoperla sinica* (Tjeder) and *Chrysopa pallens* larvae to *Aleurocan spinfetus* (Quaintance) nymphs. *Chin J Appl Entomol* **55**:217–222 (2018).
37 Chen ZZ, Zhao N, Yin XC, Zhang F and Xu YY, Physiological and biochemical changes in naturally overwintering adults of *Chrysoperla sinica* (Neuroptera: Chrysopidae) during diapause termination under two different photoperiods. *Acta Entomol Sin* **56**:120–130 (2013).
38 Wang X, Kong X, Liu SY, Huang HY, Chen ZZ and Xu YY, Selection of reference genes for quantitative real-time PCR in *Chrysoperla nipponensis* (Neuroptera: Chrysopidae) under tissues in reproduction and diapause. *J Insect Sci* **20**:20 (2020).
39 Xu YY, Hu C, Mu JY, Xu HF and Wang HG, Relationship between adult diapause development and over-wintering coloration changes in *Chrysoperla sinica* (Neuroptera). *Acta Ecol Sin* **22**:1275–1280 (2002).
40 Kang ZW, Liu FH, Pang RP, Tian HG and Liu TX, Effect of sublethal doses of imidacloprid on the biological performance of aphid endoparasitoid *Aphidius gifuensis* (Hymenoptera: Aphidiidae) and influence on its related gene expression. *Front Physiol* **9**:1729 (2018).
41 Kang ZW, Tian HG, Liu FH, Liu X, Jing XF and Liu TX, Identification and expression analysis of chemosensory receptor genes in an aphid endoparasitoid *Aphidius gifuensis*. *Sci Rep* **7**:3939 (2017).
42 Kong X, Li ZX, Gao YQ, Liu FH, Chen ZZ, Tian HG *et al*., Genome-wide identification of neuropeptides and their receptors in an aphid endoparasitoid wasp, Aphidius gifuensi. *Insects* **12**:745 (2021).
43 Liu FH, Wickham JD, Cao QJ, Lu M and Sun JH, An invasive beetle-fungus complex is maintained by fungal nutritional-compensation mediated by bacterial volatiles. *ISME J* **14**:2829–2842 (2020).
44 Kang ZW, Liu FH, Tian HG, Zhang M, Guo SS and Liu TX, Evaluation of the reference genes for expression analysis using quantitative real-time polymerase chain reaction in the green peach aphid, Myzus persicae. *Insect Sci* **24**:222–234 (2017).
45 Li YP, Zhang ZL, Robinson GE and Palli SR, Identification and characterization of a juvenile hormone response element and its binding proteins. *J Biol Chem* **282**:37605–37617 (2007).
46 Zhao LQ, Wang W, Qiu Y and Torson AS, Physiological mechanisms of variable nutrient accumulation patterns between diapausing and non-diapausing fall webworm (lepidoptera: Arctiidae) pupae. *Environ Entomol* **50**:1158–1165 (2021).
47 Zhu L, Tian Z, Guo S, Liu W, Zhu F and Wang XP, Circadian clock genes link photoperiodic signals to lipid accumulation during diapause preparation in the diapause-destined female cabbage beetles *Colaphellus bowringi*. *Insect Biochem Mol Biol* **104**:1–10 (2019).
48 Dworschak K, Gruppe A and Schopf R, Survivability and post-diapause fitness in a scolytid beetle as a function of overwintering developmental stage and the implications for population dynamics. *Ecol Entomol* **39**:519–526 (2014).
49 Goto SG, Roles of circadian clock genes in insect photoperiodism. *Entomol Sci* **16**:1–16 (2013).
50 Ikeno T, Ishikawa K, Numata H and Goto SG, Circadian clock gene clock is involved in the photoperiodic response of the bean bug *Riptortus pedestris*. *Physiol Entomol* **38**:157–162 (2013).
51 Meuti ME, Stone M, Ikeno T and Denlinger DL, Functional circadian clock genes are essential for the overwintering diapause of the Northern house mosquito, Culex pipiens. *J Exp Biol* **218**:412–422 (2015).
52 Schiesari L, Andreatta G, Kyriacou CP, O'Connor MB and Costa R, The insulin-like proteins dILPs-2/5 determine diapause inducibility in *drosophila*. *PLoS One* **11**:e0163680 (2016).
53 Pan X, Pei YF, Zhang CC, Huang YL, Chen L, Wei LQ *et al*., Effect of insulin receptor on juvenile hormone signal and fecundity in *Spodoptera litura* (F.). *Insects* **13**:701 (2022).
54 Tu MP, Yin CM and Tatar M, Mutations in insulin signaling pathway alter juvenile hormone synthesis in *Drosophila melanogaster*. *Gen Comp Endocrinol* **142**:347–356 (2005).
55 Zhu L, Yin TY, Sun D, Liu W, Zhu F, Lei CL *et al*., Juvenile hormone regulates the differential expression of putative juvenile hormone esterases via methoprene-tolerant in non-diapause-destined and diapause-destined adult female beetle. *Gene* **627**:373–378 (2017).
56 Tian Z, Guo S, Li JX, Zhu F, Liu W and Wang XP, Juvenile hormone biosynthetic genes are critical for regulating reproductive diapause in the cabbage beetle. *Insect Biochem Mol Biol* **139**:103654 (2021).
57 Guo S, Tian Z, Wu QW, King-Jones K, Liu W, Zhu F *et al*., Steroid hormone ecdysone deficiency stimulates preparation for photoperiodic reproductive diapause. *PLoS Genet* **17**:e1009352 (2021).
58 Poupardin R, Schottner K, Korbelova J, Provaznik J, Dolezel D, Pavlinic D *et al*., Early transcriptional events linked to induction of diapause revealed by RNAseq in larvae of drosophilid fly, Chymomyza costata. *BMC Genomics* **16**:720 (2015).
59 Ogihara MH, Ikeda H, Yamada N, Hikiba J, Nakaoka T, Fujimoto Y *et al*., Identification of ecdysteroidogenic enzyme genes and their expression during pupal diapause in the cabbage armyworm, Mamestra brassicae. *Insect Mol Biol* **26**:286–297 (2017).
60 Guney G, Toprak U, Hegedus DD, Bayram S, Coutu C, Bekkaoui D *et al*., A look into Colorado potato beetle lipid metabolism through the lens of lipid storage droplet proteins. *Insect Biochem Mol Biol* **133**:103473 (2021).

61 Xiang M, Zhang HZ, Jing XY, Wang MQ, Mao JJ, Li YY *et al*., Sequencing, expression, and functional analyses of four genes related to fatty acid biosynthesis during the diapause process in the female ladybird, *Coccinella septempunctata* L. *Front Physiol* **12**:706032 (2021).
62 Robich RM and Denlinger DL, Diapause in the mosquito *Culex pipiens* evokes a metabolic switch from blood feeding to sugar gluttony. *Proc Natl Acad Sci U S A* **102**:15912–15917 (2005).
63 Reynolds JA, Poelchau MF, Rahman Z, Armbruster PA and Denlinger DL, Transcript profiling reveals mechanisms for lipid conservation during diapause in the mosquito, Aedes albopictus. *J Insect Physiol* **58**:966–973 (2012).
64 Zhang XX, Yang S, Zhang XM, Wang S, Zhang JH and Xi JH, TMT-based quantitative proteomic profiling of overwintering *Lissorhoptrus oryzophilus*. *Front Physiol* **10**:1623 (2019).

